

Expansion of scattering length in S -matrix poles and the phenomenon of resistant virtual statesRoman Čurík^{✉*} and Michal Tarana^{✉†}*J. Heyrovský Institute of Physical Chemistry of the ASCR, v.v.i., Dolejškova 2155/3, 182 23 Prague 8, Czech Republic*

Jiří Horáček

Faculty of Mathematics and Physics, Charles University, V Holešovičkách 2, 18000 Prague 8, Czech Republic

(Received 11 May 2023; accepted 23 June 2023; published 11 July 2023)

A simple expansion of the scattering length in terms of S -matrix poles is derived for the angular momenta $l > 0$. This expression shows that the dominant role in the low-energy collisions is played by the poles lying close to the origin of the complex momentum plane. Among these poles a peculiar class of virtual states is found to respond very weakly to the scaled perturbation potentials and thus resistant to producing trajectories in the complex momentum plane. Properties and an impact on low-energy collisions of these resistant virtual states are discussed.

DOI: [10.1103/PhysRevA.108.012807](https://doi.org/10.1103/PhysRevA.108.012807)**I. INTRODUCTION**

Most of what is known about interactions between particles in the microworld has been established by means of collision processes. The scattering length is the primary parameter for a quantum description of a collision of two bodies in the low-energy limit. As such, it has been intensively studied in a number of domains of quantum physics. In nuclear physics the scattering length is utilized to describe properties of nuclear halo states within the effective field theory [1]. Besides the most occurring and studied s -state halo nuclei, there are nuclear systems where the scattering length for the higher partial waves of the neutron-nuclei collisions becomes important. The p -wave scattering length was employed in the modeling of elastic $n\alpha$ collisions [2], while the halo nuclei ^{15}C and ^{17}C are described by the d -wave scattering length [3].

In the field of atomic and molecular physics, Feshbach resonances have found many applications in ultracold gases, where their presence allows for a fine tuning of the scattering length by electric and magnetic fields. Again, the vast majority of these elastic-threshold resonances are in the s wave. However, there are systems with the $l = 1, 2$ entrance channels known in the μK domain [4]. Furthermore, the s - and p -wave scattering lengths appear in the well-known low-density expansions for the ground-state energy of many-boson and many-fermion systems [5].

In the experiments that involve electron-molecule collisions at low energies (below 1 eV), the scattering length can be determined from the forward-backward anisotropy of the measured cross sections [6,7]. In these experiments the large and negative scattering length is often explained by the presence of a virtual state. From a theoretical point of view, the virtual state is represented by a pole of the scattering S matrix

that is located close to the origin, on the negative imaginary axis in the complex momentum plane. A presence of virtual states in the elastic $e^- + \text{CO}_2$ scattering has been demonstrated in a number of calculations [8–12]. An enhancement of the electron-impact vibrational excitation of molecules via a virtual state has frequently been discussed in the literature, mainly in connection with the elastic and inelastic threshold peaks [13–17]. Dvořák *et al.* [18,19] have shown that the impact of the virtual state on the vibrationally inelastic collisions can extend up to several electronvolts of collision energies through its coupling to the higher-lying resonant state. Note that the virtual states involved in all the references above possess the s -wave character.

For more than half of a century there have been attempts to establish a link between the S -matrix poles and the parameters of the effective range theory. The early work of Demkov and Drukarev [20] discussed a two-pole approximation to the S matrix. This approximation also employs a background phase to correct for all the other poles not included in the model. While the resulting s -wave scattering length was linked to the imaginary components of the two poles, the unknown background phase could not be ruled out. The later studies of $e + \text{CO}_2$ collisions [8,12] neglected the background phase and assumed that the s -wave scattering length a_0 can be simply computed from a single pole $i\kappa$, lying on the imaginary momentum axis, as $a_0 = 1/\kappa$.

An important contribution to this search of the link between the S -matrix poles and the effective range parameters was made by Tolstikhin *et al.* [21] and their theory of s -wave Siegert pseudostates (SPSs), later generalized for higher angular momenta [22]. The theory was developed to solve the spherical Hamiltonian problem inside a finite volume in terms of complex eigenstates and eigenvalues of the momentum. Authors demonstrated [22] that the s -wave scattering length a_0 does not depend solely on the imaginary components of the the poles reciprocals but also on the box size r_0 , akin to the background phase of Demkov and Drukarev [20].

*roman.curik@jh-inst.cas.cz

†michal.tarana@jh-inst.cas.cz

In the first part of this paper we focus on an extension of the work of Batishchev and Tolstikhin [22] in which we derive a simple formula for an expansion of the scattering length solely in terms of the S -matrix poles, for $l > 0$. The formula will show that the poles close to the origin possess a dominant impact on the scattering length. This is in contrast to the s -wave case derived by Batishchev and Tolstikhin [22]. The second part of this paper discusses properties of such poles, with a focus on the poles lying on the negative imaginary axis, i.e., virtual states. It is shown that there exists a class of peculiar virtual states that resist producing trajectories in the momentum plane upon application of a scaled perturbation potential. We call these states resistant virtual states (RVSs).

Throughout the rest of this paper, the virtual states and bound states are characterized by their momenta k rather than energies $E = k^2/2$. This is convenient, since the momenta are purely imaginary ($k = i\kappa$, $\kappa \in \mathbb{R}$), where $\kappa > 0$ for the bound states and $\kappa < 0$ for the virtual states. Unless stated otherwise, the atomic units are used throughout the rest of this paper.

II. SIEGERT STATES

The virtual states discussed in this article belong to a broader category of Siegert states [23]. A theory of these states formulated by Tolstikhin *et al.* [21] and later generalized by Batishchev and Tolstikhin [22] is reviewed in this section with an emphasis on those aspects that are important in the context of virtual states.

The potential $V(r)$ considered in this paper is spherically symmetric and has a finite range, $V(r > r_0) \equiv 0$, or it decays beyond r_0 sufficiently rapidly with increasing r that the effect of the tail on the scattering quantities is negligible. The Siegert states are such solutions $\phi_k(r)$ of the Schrödinger equation

$$\left[-\frac{1}{2} \frac{d^2}{dr^2} + \frac{l(l+1)}{2r^2} + V(r) \right] \phi_k(r) = \frac{k^2}{2} \phi_k(r) \quad (1)$$

that are regular at the origin [$\phi_k(0) = 0$] and satisfy the asymptotic outgoing-wave boundary condition

$$\left(\frac{d}{dr} - ik \right) \phi_k(r) \Big|_{r \rightarrow \infty} = 0. \quad (2)$$

The partial wave $l \geq 0$ is fixed, otherwise arbitrary. The eigenstates that satisfy Eq. (2) include all the bound, resonant, and virtual states of the potential $V(r)$. Their eigenmomenta k are pure positive imaginary for the bound states, pure negative imaginary for the virtual states, and complex for the resonances. The significance of these states is that the eigenvalues k correspond to the poles of the scattering matrix in the complex k plane [24].

A. Siegert pseudostates

Tolstikhin *et al.* [21] developed a method to accurately approximate the s -wave Siegert states by enforcing the boundary condition with the same form as in Eq. (2), however, at a finite $r \geq r_0$ rather than at infinity. The solutions of the Eqs. (1) and (2) obtained in this way are referred to as Siegert pseudostates (SPSs). This approach cannot be applied in a straightforward manner for $l > 0$. The presence of the centrifugal barrier beyond r_0 causes the difference between

the asymptotic character of $\phi_k(r)$ and its form at any finite $r \geq r_0$.

The theory of SPSs for $l > 0$ was developed by Batishchev and Tolstikhin [22]. The solution $\phi_k(r)$ that meets the asymptotic boundary condition (2) is expressed at a finite value of $r \geq r_0$ in terms of the spherical Hankel function $h_l^{(1)}(z)$ [25] as

$$\phi_k(r)|_{r \geq r_0} \propto kr h_l^{(1)}(kr). \quad (3)$$

Then an introduction of the function

$$e_l(z) = e^{iz} \frac{\theta_l(-iz)}{(-iz)^l}, \quad (4)$$

where θ_l are the reverse Bessel polynomials [26], allows for an application of a boundary condition at finite r that is equivalent to Eq. (2). The function $e_l(z)$, up to a constant phase factor, coincides with $z h_l^{(1)}(z)$ [26]. At the same time, its logarithmic derivative satisfies the equation

$$\frac{1}{e_l(z)} \frac{de_l(z)}{dz} = i - \frac{1}{z} \sum_{p=1}^l \frac{z_{lp}}{iz + z_{lp}}, \quad (5)$$

where z_{lp} is the p th root of the reverse Bessel polynomial $\theta_l(z)$ [22]. This directly yields the boundary condition at a finite r :

$$\left(\frac{d}{dr} - ik + \frac{1}{r} \sum_{p=1}^l \frac{z_{lp}}{ikr + z_{lp}} \right) \phi_k(r) \Big|_{r \geq r_0} = 0. \quad (6)$$

This “pull-back” of the boundary condition allows for accurate numerical calculations of the SPSs using the expansion of $\phi_k(r)$ in a finite basis set without the necessity of its extension beyond the range of $V(r)$. In a special case of $l = 0$, the last term in the parentheses on the left-hand side of Eq. (6) vanishes and the form of the boundary condition becomes identical to that of Eq. (2).

The solution of Eq. (1) on a finite interval $(0, r_0)$, employing a finite basis set, results in a set of discrete eigenmomenta k_n and corresponding eigensolutions $\phi_n(r) \equiv \phi_{k_n}(r)$. These SPSs are double complete on the space spanned by the given basis set, and they can be orthonormalized with a scalar product [22]:

$$\int_0^{r_0} \phi_n(r) \phi_m(r) dr + i \frac{\phi_n(r_0) \phi_m(r_0)}{k_n + k_m} \times \left[1 + \sum_{p=1}^l \frac{z_{lp}}{(ik_n r_0 + z_{lp})(ik_m r_0 + z_{lp})} \right] = \delta_{nm}. \quad (7)$$

III. SCATTERING LENGTH

According to the Wigner threshold law [27], the phase shift $\delta_l(k)$ behaves at the low collision energies as

$$\delta_l(k) \xrightarrow{k \rightarrow 0} -(a_l k)^{2l+1}. \quad (8)$$

The parameter a_l is the scattering length for a given partial wave l . The aim of this section is to show how the low-energy scattering parameter a_l can be expressed in terms of the S -matrix poles. The formal framework for the derivation that will follow is the Siegert pseudostate theory of Batishchev

and Tolstikhin [22]. The authors have demonstrated that the scattering matrix S can be written in terms of the SPS poles as

$$S_l(k) = e^{2i\delta_l(k)} = e^{-2ikr_0} \prod_{n=1}^{2N+l} \frac{k_n + k}{k_n - k}. \quad (9)$$

The finite basis of N elements on the radial interval $(0, r_0)$ provides exactly $2N + l$ SPSs. Furthermore, Batishchev and Tolstikhin [22] have derived a general formula for the scattering length

$$a_l^{2l+1} = -\frac{r_0^{2l+1}}{\theta_l^2(0)} \left[\frac{-1}{2l+1} + \frac{1}{2r_0} \sum_{n=1}^{2N+l} \frac{\phi_n^2(r_0)}{k_n^2} \right], \quad (10)$$

where $\phi_n(r_0)$ are the surface values of the SPSs and the $\theta_l(z)$ denote the above mentioned reverse Bessel polynomials [26]. In our experience those formulas that involve surface values of the SPSs appear to be unstable, probably due to the fact that most of these states exponentially grow. This weakness can be easily remedied by use of Eq. (66) of Ref. [22], which allows us to rewrite the scattering length into

$$a_l^{2l+1} = \frac{r_0^{2l+1}}{(2l+1)\theta_l^2} + (-1)^{l+1} \sigma_{2l+1}(x_i), \quad (11)$$

where $\sigma_k(x_i)$ is the elementary symmetric polynomial of the order k in variables x_i [28], and the abbreviation $\theta_l \equiv \theta_l(0)$ will be used henceforth. The set of variables x_i is a union of two subsets [22] defined as

$$\underbrace{x_1, x_2, \dots, x_{2N+l}}_{\frac{1}{\lambda_1}, \frac{1}{\lambda_2}, \dots, \frac{1}{\lambda_{2N+l}}}, \underbrace{x_{2N+l+1}, \dots, x_{2N+2l}}_{\frac{r_0}{z_{l1}}, \dots, \frac{r_0}{z_{ll}}}, \quad (12)$$

where λ_n are related to the Siegert poles $\lambda_n = ik_n$ and $\{z_{lp}, p = 1, \dots, l\}$ is a set of l roots of the reverse Bessel polynomial $\theta_l(z)$. Note that the scattering length (11) is written in terms of the box size r_0 , of roots z_{lp} , and of the S -matrix poles λ_n . In the following we aim to demonstrate that the fundamental physical quantity a_l , defining the collisions at the low energies, should and will depend only on the S -matrix poles λ_n .

A. Symmetric polynomials

The elementary symmetric polynomials $\sigma_k(x_i)$ are defined as follows [28]:

$$\begin{aligned} \sigma_0(x_1, \dots, x_n) &= 1, \\ \sigma_1(x_1, \dots, x_n) &= \sum_{1 \leq i \leq n} x_i, \\ \sigma_2(x_1, \dots, x_n) &= \sum_{1 \leq i < j \leq n} x_i x_j, \\ &\vdots \end{aligned} \quad (13)$$

The last identity required here from the Ref. [22] [Eq. (64) from the reference] states that

$$\begin{aligned} \sigma_{2s+1}(x_1, \dots, x_{2(N+l)}) &= 0, \quad s = 0, 1, \dots, l-1, \\ l &> 0. \end{aligned} \quad (14)$$

The physical interpretation of the identity is following. Equation (9) shows, that for a given angular momentum l , the S

matrix $S_l(k)$ and hence the phase shift $\delta_l(k)$ can be computed solely from the Siegert poles k_n (or $\lambda_n \equiv ik_n$). However, the Wigner threshold law (8) dictates that all the coefficients a_s^{2s+1} in front of the k^{2s+1} with $s < l$ should vanish. This property is not satisfied by an arbitrary set of Siegert poles k_n in Eq. (9). Therefore, the distribution of the Siegert poles in the complex plane cannot be arbitrary, and it must satisfy l conditions. We will see that these conditions are represented by Eq. (14).

Another kind of the symmetric polynomials, which will be employed in the present derivation, is the sum of powers

$$s_k(x_1, \dots, x_n) = \sum_{i=1}^n x_i^k. \quad (15)$$

The Fundamental Theorem on Symmetric Polynomials [28] states that every symmetric polynomial (for example, the power-sum polynomial s_k) can be expressed uniquely as a polynomial in the elementary symmetric polynomials $\sigma_1, \dots, \sigma_k$. Generally, the decomposition into the elementary symmetric polynomials may be a complicated process, but in the case of the symmetric polynomial s_k it is streamlined by one of the Newton formulas [28,29]

$$k\sigma_k = \sum_{r=1}^k (-1)^{r-1} s_r \sigma_{k-r}, \quad k = 1, 2, 3, \dots, \quad (16)$$

which can be used recursively, starting with $s_1 = \sigma_1$.

B. Roots of Bessel polynomials

Roots of the Bessel polynomials play an important role in a wide variety of the research, e.g., in the signal processing [30], statistics [31], theory of differential equations [32], etc. In the present study these roots enter the starting formula (11) for the scattering length through the variables x_i defined in (12). While the roots of the reverse Bessel polynomials $\theta_l(z)$ are denoted as z_{lp} , the roots of the Bessel polynomials $y_l(z)$ are simply the reciprocals $1/z_{lp}$. This can be easily seen from the relation between the polynomials

$$\begin{aligned} y_l(z) &= z^l \theta_l(1/z) = \prod_{p=1}^l (1 - z z_{lp}) = \prod_{p=1}^l (-z_{lp}) \left(z - \frac{1}{z_{lp}} \right) \\ &= \theta_l \prod_{p=1}^l \left(z - \frac{1}{z_{lp}} \right). \end{aligned} \quad (17)$$

Furthermore, the product formula (17) leads to a polynomial expression, in which the coefficients are essentially the elementary symmetric polynomials [28] of the roots $1/z_{lp}$:

$$y_l(z) = \theta_l \sum_{m=0}^l (-1)^{l-m} \sigma_{l-m}(1/z_{lp}) z^m = \sum_{m=0}^l \frac{(l+m)!}{m!(l-m)!} \left(\frac{z}{2} \right)^m. \quad (18)$$

The last identity is the known definition of the Bessel polynomials [33]. By comparing the coefficients on both sides of the polynomial equality (18), the symmetric elementary polynomials of the set of $1/z_{lp}$ roots can be evaluated as

$$\sigma_k(1/z_{lp}) = \frac{(-1)^k}{\theta_l} \frac{(2l-k)!}{k!(l-k)! 2^{l-k}}. \quad (19)$$

The first two orders of the above equation give

$$k = 0 : \theta_l(0) = \frac{(2l)!}{l!2^l} = (2l - 1)!!, \quad (20)$$

$$k = 1 : \sigma_1(1/z_{lp}) = \sum_{p=1}^l \frac{1}{z_{lp}} = -1. \quad (21)$$

An identity similar to Eq. (19) but for the sum-of-power polynomials s_k has been reported previously [31]:

$$s_{2s+1}(1/z_{lp}) = \sum_{p=1}^l \frac{1}{z_{lp}^{2s+1}} = \begin{cases} 0, & 0 < s < l \\ \frac{(-1)^l}{\theta_l^2}, & s = l \end{cases}. \quad (22)$$

The case of $s = 0$ is covered by Eq. (21), and the case of $s > l$ can be found in Refs. [31,34], but is of no relevance for the present work.

C. Scattering length for $l > 0$

The s -wave scattering length has been reported previously [22], and it can be easily derived from Eq. (11)

$$a_0 = r_0 - \sum_n \frac{1}{\lambda_n} = r_0 + \sum_n \frac{i}{k_n}. \quad (23)$$

On the other hand, for the higher partial waves $l > 0$, the $s = 0$ condition (14) implies that

$$\sigma_l(x_i) = \sigma_1(1/\lambda_i) + \sigma_1(r_0/z_{lp}) = 0, \quad l > 0, \quad (24)$$

and therefore with the use of (21) we have

$$r_0 = \sigma_1(1/\lambda_i) = s_1(1/\lambda_i) = \sum_n \frac{1}{\lambda_n}, \quad l > 0. \quad (25)$$

This expression clearly states that the leading term ($-a_0k$) on the r.h.s. of Eq. (8) vanishes for the partial waves with $l > 0$.

The scattering length for the higher partial waves can be computed from Eq. (11)

$$(2l + 1)a_l^{2l+1} = \frac{r_0^{2l+1}}{\theta_l^2} + (-1)^{l+1}(2l + 1)\sigma_{2l+1}(x_i). \quad (26)$$

The second term on the r.h.s. can be expanded by employing the Newton formula (16) with the reversed order as

$$(2l + 1)\sigma_{2l+1}(x_i) = \sum_{k=0}^{2l} (-1)^k s_{2l+1-k} \sigma_k. \quad (27)$$

In the above equation, and in the following text, the symmetric polynomials σ_k and s_k without explicit arguments always denote the polynomials $\sigma_k(x_i)$ and $s_k(x_i)$, respectively.

Before the general version we start with an illustration for the $l = 1$ case of Eqs. (26) and (27). In this particular case we have

$$3a_1^3 = \frac{r_0^3}{\theta_1^2} + \underbrace{(s_3 - s_2\sigma_1 + s_1\sigma_2)}_{3\sigma_3}. \quad (28)$$

The last two terms in the equation vanish because $\sigma_1(x_i) = s_1(x_i) = 0$ as stated in Eq. (24). Furthermore,

$$s_3(x_i) = s_3(1/\lambda_i) + s_3(r_0/z_{lp}) = s_3(1/\lambda_i) - \frac{r_0^3}{\theta_1^2}, \quad (29)$$

where the last equality utilized the result (22). Therefore the p -wave scattering length can be written in terms of the Siegert pseudostate poles as

$$3a_1^3 = s_3(1/\lambda_i) = \sum_n \frac{1}{\lambda_n^3} = \sum_n \frac{i}{k_n^3}. \quad (30)$$

Note that expression (28) is valid only for $l = 1$, as the angular momentum l defines the arguments of the polynomials σ_k and s_k through the poles λ_n and the roots z_{lp} . For $l > 1$, the term $3\sigma_3(x_i)$, represented by the parentheses in (28), vanishes due to conditions (14). Since $s_3(r_0/z_{lp}) = 0$ for $l > 1$, as stated in (22), the $s_3(1/\lambda_i)$ must also vanish for $l > 1$. This property will propagate for higher l values as will be demonstrated below.

The general case starts with the expansion (27) written as

$$(2l + 1)\sigma_{2l+1} = s_{2l+1} - s_{2l}\sigma_1 + \dots - s_2\sigma_{2l-1} + s_1\sigma_{2l}. \quad (31)$$

The symmetric polynomials here are computed for the λ_i eigenmomenta and z_{lp} roots that are tied to the angular momentum value l . Due to this all the terms on the r.h.s of Eq. (31) except the first s_{2l+1} vanish because one of these two cases apply:

(a) The vanishing terms contain the odd order of the symmetric elementary polynomial σ_{2s+1} with $s < l$. In this case the condition (14) is responsible for their disappearance.

(b) The vanishing terms contain the odd order of the symmetric powers-sum polynomial s_{2s+1} with $s < l$. The zero value of these polynomials is less trivial and must be built by the induction process that employs a lower order version of Eq. (31),

$$\begin{aligned} 0 &= (2s + 1)\sigma_{2s+1} \\ &= s_{2s+1} - s_{2s}\sigma_1 + \dots - s_2\sigma_{2s-1} + s_1\sigma_{2s}, \quad s < l, \end{aligned} \quad (32)$$

which is valid for all $s < l$:

$$\begin{aligned} s = 1 : \quad 0 &= s_3 - s_2\sigma_1 + s_1\sigma_2, \\ s = 2 : \quad 0 &= s_5 - s_4\sigma_1 + s_3\sigma_2 - s_2\sigma_3 + s_1\sigma_4, \\ &\vdots \\ s = l - 1 : \quad 0 &= s_{2l-1} - \dots + s_1\sigma_{2l-2}. \end{aligned} \quad (33)$$

The induction starts with $s_1(x_i) = \sigma_1(x_i) = 0$ and employs the statement (a) above. The power-sum polynomials s_{2s+1} can be split to two parts as

$$0 = s_{2s+1}(x_i) = s_{2s+1}(1/\lambda_i) + s_{2s+1}(r_0/z_{lp}), \quad \text{for } s < l, \quad (34)$$

and because of properties (20) the term

$$s_{2s+1}(1/\lambda_i) = 0, \quad \text{for } s < l. \quad (35)$$

Since one of the above cases (a) or (b) always applies for all but the first term in Eq. (31), only the leading term contributes:

$$(2l + 1)\sigma_{2l+1} = s_{2l+1}(1/\lambda_i) + r_0^{2l+1} s_{2l+1}(1/z_{lp}). \quad (36)$$

The properties (20) allow us to evaluate the second term on the r.h.s. of Eq. (36) as $s_{2l+1}(1/z_{lp}) = (-1)^l/\theta_l^2$. Such identity simplifies the expression (26) to the final formula

$$(2l + 1)a_l^{2l+1} = (-1)^{l+1} s_{2l+1}(1/\lambda_i). \quad (37)$$

With a more physical language, the $(2l + 1)$ -power of the l -wave scattering length can be written in terms of the S -matrix poles $\lambda_n \equiv ik_n$ as

$$(2l + 1)a_l^{2l+1} = (-1)^{l+1} \sum_n \frac{1}{\lambda_n^{2l+1}} = \sum_n \frac{i}{k_n^{2l+1}}, \quad l > 0, \quad (38)$$

or finally

$$a_l^{2l+1} = \frac{1}{2l + 1} \sum_n \frac{i}{k_n^{2l+1}}, \quad l > 0. \quad (39)$$

Note that the s -wave version (23) depends explicitly on the box size r_0 , while this parameter disappears from the explicit formula (39). However, the implicit dependence on the box size remains, since the Siegert-pseudostate poles k_n describe not only the physical resonances but also the discretized continuum spectrum, so-called box states. In situations, frequently encountered in atomic and molecular physics, where only a few poles appear near the threshold, a few-pole approximation of Eq. (39) provides a convenient way to calculate the scattering length.

Recently we have found that the scattering-length formula (39) can also be derived in an alternative and simpler way by employing some of the ideas from Ref. [35].

IV. RESISTANT VIRTUAL STATES

While the effect of the low-energy resonances and weakly bound states on the low-energy scattering has been extensively explored, the role of the virtual states has so far been understood primarily on a qualitative level. According to Eq. (39), valid for $l > 0$, a virtual state near the threshold can significantly affect the low-energy scattering as well.

To the best of our knowledge, the related studies have been exclusively focused on the virtual states in the s wave, unanimously concluding that their presence near the threshold causes a large low-energy scattering cross section. However, its quantification has been limited. Batishchev and Tolstikhin [22] formulated the first analytical expression that accurately quantifies this influence for $l = 0$, and Eq. (39) is its equivalent for the higher partial waves. As is shown below, it is not difficult to find an interaction, the scattering length of which is in the p -wave predominately determined by the near-threshold virtual state and all the remaining poles form only a small correction. The validity of Eq. (39) is general within the scope of the short-range interactions, and it can be applied to electron collisions with atoms or molecules. It provides a convenient way of calculation of the scattering length in cases of dominant near-threshold poles.

To demonstrate this effect, the S -matrix poles near the threshold in the p -wave were calculated for a short-range potential by Davis and Sommerfeld [36]. As is discussed below, this calculation revealed that the character of the virtual state providing a dominant contribution to the scattering length is unusual. Usually the S -matrix poles for a local potential appear in pairs. A bound state with a positive imaginary momentum is paired with a virtual state on the negative imaginary axis [37]. For a resonance in the fourth quadrant of the complex momentum plane, another pole in the third quadrant exists, symmetrically with respect to the imaginary

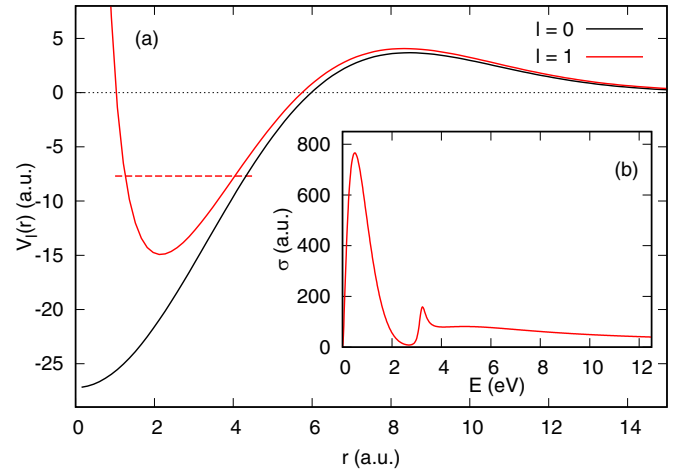


FIG. 1. (a) The potential in Eq. (40). The solid black and red (gray) lines correspond to the angular momenta $l = 0$ and $l = 1$, respectively. The red (gray) dashed line illustrates the energy of the p -wave bound state. (b) The elastic scattering cross section in the p wave as a function of the energy is plotted.

axis. These pairs move along the trajectories in the complex momentum plane as the overall strength of the interaction changes. With the potential becoming increasingly more attractive, the resonance pair symmetrically moves towards the origin (for $l > 0$), where it splits and forms a pair of the bound and virtual state, moving away from each other as the interaction further becomes more attractive.

All the calculated poles of the p -wave S -matrix of the potential studied below [36], except one, follow this pattern. One virtual state appears without any associated bound state. In an attempt to identify its partner, its trajectory in the complex momentum plane was studied as a function of the scaling factor in front of the potential. As is shown below, this virtual state not only appears without any corresponding bound state, furthermore, its position on the negative imaginary axis is only very weakly affected by the modification of the potential depth. In terms of Eq. (39), this state represents the dominant contribution to the scattering length. More detailed study revealed that this unusual virtual state exists for a broad variety of short-range potentials, and it has not been previously characterized. It will be referred to as the *resistant virtual state* (RVS).

A. Model potential

In order to compare various methods for calculation of resonances, Davis and Sommerfeld [36] studied the electron scattering off the potential

$$V_l(r) = V(r) + \frac{l(l+1)}{2r^2}, \quad (40)$$

where

$$V(r) = (ar^2 - b)e^{-cr^2} \quad (41)$$

and $a = 0.028$, $b = 1$, and $c = 0.028$. This potential is plotted in Fig. 1 for the angular momenta $l = 0, 1$. Their study was restricted to the elastic scattering in the p wave where a shape resonance exists at energy $E_R = 3.17$ eV that has width

TABLE I. Energies (in eV) of the bound state, virtual state, and low-energy resonances of the potential (40) in the partial waves p , d , and f .

State	p wave		d wave		f wave	
	E_R	Γ	E_R	Γ	E_R	Γ
Bound	-7.1705	0.0	-0.4921	0.0	-	-
Virtual	-7.1704	0.0	-0.4930	0.0	-	-
	-0.0977	0.0	-	-	-0.469	0.0
Resonance	3.1730	0.3216	6.484	3.029	5.001	0.258

$\Gamma = 0.32$ eV. In addition, this potential supports a bound state with the energy $E_B = -7.17$ eV. The calculated p -wave cross section is shown in the inset of Fig. 1. The cross section is dominated by a high peak at around 1 eV; the resonance peak at 3.2 eV represents a relatively small feature as compared to the threshold peak. In addition, this potential also supports a virtual state with very small energy ≈ -98 meV that is not mentioned by Davis and Sommerfeld [36]. The positions of the resonances as well as the virtual states were obtained by solving the Lippmann-Schwinger equation on the unphysical sheet [38] (see the Appendix).

B. Trajectories of virtual states

As can be seen in Table I, the potential (40) supports a single bound state and two virtual states. The question we would like to address here is how the imaginary momenta of the virtual states change with the overall strength of the potential and whether the virtual state that is not associated with a bound state can leave the negative imaginary momentum semiaxis.

To this end, we introduce a real factor Λ that scales the model potential (41),

$$W_l(r) = \Lambda V(r) + \frac{l(l+1)}{2r^2}, \quad (42)$$

and calculate the imaginary momenta of the bound and virtual states for different values of Λ . While for one virtual state, the momentum significantly depends on the potential strength, it only very weakly changes for the other, even at $\Lambda \rightarrow \infty$. On the the energy scale, the energy of the near-threshold virtual state changes only from about -98 meV to -55 meV and remains unchanged with further increase of the potential strength. Due to this “resistance,” this state will be referred to as the RVS.

Figure 2 displays the imaginary momenta κ of the bound and virtual states as a function of Λ . In addition to the bound state and RVS, a second virtual state exists that develops almost symmetrically to the bound state. It merges with the bound-state curve as Λ decreases and both states turn into a pair of resonances (not shown in Fig. 2) at $\Lambda \approx 0.46$. Only one state appears on the imaginary k axis for $\Lambda \lesssim 0.46$ —the RVS.

As the value of Λ raises, excited bound states appear along with the corresponding virtual states. These exhibit a series of very narrow avoided crossings with the RVS. Details of the first crossing are shown in the inset of Fig. 2.

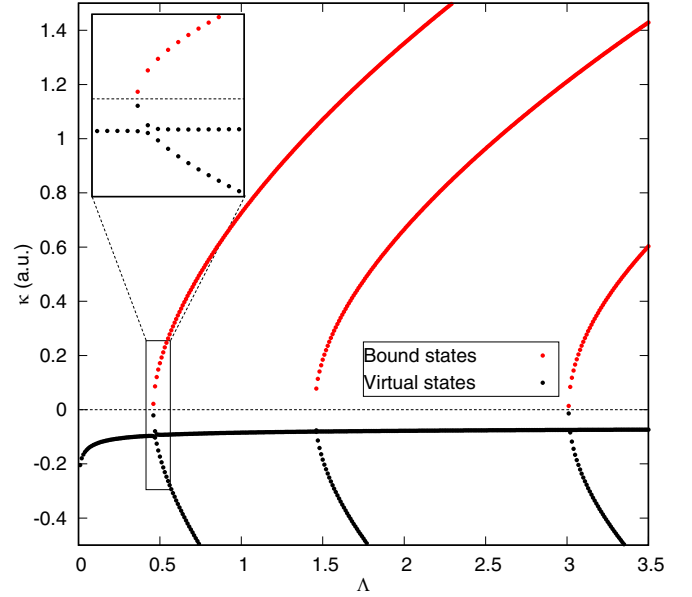


FIG. 2. Imaginary momentum $\kappa = -ik$ as a function of the dimensionless scaling parameter Λ [see Eq. (42)] in the partial wave p . The unperturbed potential (40) corresponds to $\Lambda = 1$. The red dots $\kappa > 0$ represent the trajectories of the bound states; the black dots $\kappa < 0$ correspond to the trajectories of the virtual states. The RVS is clearly seen.

Although the RVS presented here was calculated for the specific model potential (40) in the p wave, it appears for a wide category of the short-range potentials and for higher partial waves. Its nature is discussed in the rest of this section along with its effect on the low-energy scattering.

C. Role of RVSS in scattering

Virtual states in the s wave are known to strongly impact the elastic [6,7,9] and vibrationally inelastic [17,18] collisions of electrons with molecular targets at low collision energies. With the toolkit of the SPSs [22] we can examine the role of the p -wave RVS in the low-energy scattering, specifically the scattering by the Davis-Sommerfeld potential [36] defined by Eq. (40).

Since the SPSs $\phi_n(r)$ form a complete and orthonormal set of functions inside a finite interval $\langle 0, r_0 \rangle$, a general scattering solution $\phi_l(r, k)$, for a collision energy $E = k^2/2$, can be expressed by a linear combination of SPSs. This expansion was given by Batishchev and Tolstikhin [22] as

$$\begin{aligned} \phi_l(r, k) &= \sum_n c_n \phi_n(r) \\ &= -ike^{-ikr_0} \frac{(-ikr_0)^l}{\theta_l(-ikr_0)} \sum_n \frac{\phi_n(r_0)}{k_n(k_n - k)} \phi_n(r). \end{aligned} \quad (43)$$

The expansion coefficients c_n are complex. Their absolute values $|c_n|$ for four selected collision energies $E = 10^{-3}, 10^{-2}, 10^{-1}, 1.0$ a.u. and for the angular momentum $l = 1$ are shown in Fig. 3. There are several observations that can be made from this numerical study:

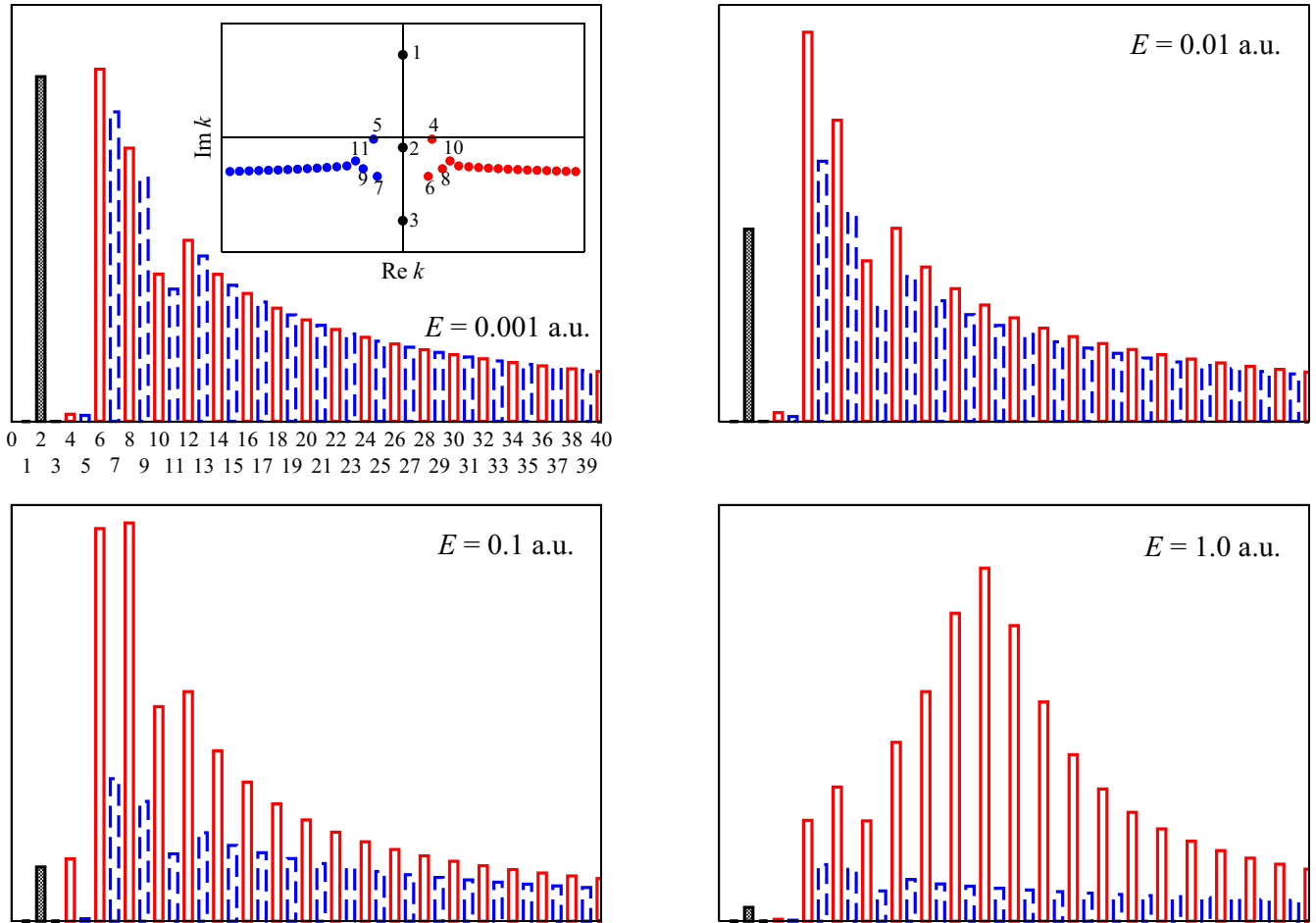


FIG. 3. Absolute values $|c_n|$ of the expansion coefficients (43) for the scattering solution at four selected collision energies E for the p wave. The contribution of the bound and antibound states is shown by black, the contributions of the outgoing- and incoming-wave SPSs are displayed by red (full gray lines) and blue (dashed gray lines), respectively. The inset in the top-left panel shows the distribution of the SPS poles that are closest to the origin. The resistant pole is marked by the number 2.

(1) At low energies $E \leq 10^{-2}$ a.u. the contribution of outgoing- and incoming-wave SPSs is very similar as the p -wave phase shift is small. That leads to an S matrix $S \sim 1$ that gives a weak phase unbalance between asymptotic incoming and outgoing waves.

(2) The RVS is the only pole from the imaginary axis contributing to the scattering wave function. This is because the scattering solutions are orthogonal to the bound space.

(3) An importance of the resistant VS increases with the decreasing collision energy as it becomes one of the dominant contributions at $E = 10^{-3}$ a.u. for this particular potential.

The expansion of the scattering length (39) in terms of the S -matrix poles offers another perspective of the role of the RVSs in the scattering. An accurate calculation of the p -wave scattering length (8) of the potential from Eq. (40) yields the value $a_1 = 8.137$ a.u. A single-pole approximation of Eq. (39) including only the RVS yields a very close value, 8.182 a.u. The RVS predominately determines the scattering physics in the threshold region where the Wigner threshold law is applicable.

The picture provided by the study of the model potential (40) can be, in the case of the more general short-range

interaction, complicated by low-energy resonances or weakly bound states and their associated virtual states. In these cases their contributions to the expansion (39) can be comparable to that of the RVS.

D. Virtual states induced by boundary condition

To understand the nature of the states in the focus of this work for an arbitrary short-range potential $V(r)$, the discussion in the rest of this section will be restricted to the imaginary k axis parameterized by κ . It is convenient to rewrite the left-hand side of Eq. (6) as a functional:

$$F_l[\kappa, \varphi_{i\kappa}(r)] = \frac{1}{\varphi_{i\kappa}(r_0)} \left. \frac{d\varphi_{i\kappa}(r)}{dr} \right|_{r=r_0} + \kappa + \frac{1}{r_0} \sum_{p=1}^l \frac{z_{lp}}{z_{lp} - \kappa r_0}, \quad (44)$$

where $\varphi_{i\kappa}(r)$ is a solution of the Schrödinger equation (1) calculated for the momentum $k = i\kappa$ that is regular at the origin [$\varphi_{i\kappa}(0) = 0$] and that is not subject to any other boundary condition, such as (2). Such solutions are related to their

derivatives at given and fixed r_0 via the R matrix [39,40]:

$$\varphi_{ik}(r_0) = R(-\kappa^2/2) \left. \frac{d\varphi_{ik}(r)}{dr} \right|_{r=r_0}, \quad (45)$$

where R is only a function of the energy. Therefore, in terms of κ , it depends on $|\kappa|$. Substitution of Eq. (45) into Eq. (44) yields a function of κ :

$$f_l(\kappa) = \frac{1}{R(-\kappa^2/2)} + \kappa + \frac{1}{r_0} \sum_{p=1}^l \frac{z_{lp}}{z_{lp} - \kappa r_0}. \quad (46)$$

Then the condition (6), specifying the momenta of the bound and virtual states, can be written as $f_l(\kappa) = 0$.

A possible (not necessarily accurate or computationally beneficial) method to calculate the bound and virtual states would be to first numerically calculate the logarithmic derivative $1/R(-\kappa^2/2)$ of the solutions of the Schrödinger equation at r_0 for a set of values of κ . This can be used to construct the function (46). Its zeros determine those values of κ that satisfy the boundary condition (6) on the imaginary axis and hence they correspond to the bound and virtual states of $V(r)$.

The nodes of $f_l(\kappa)$ are related to its poles. Since the function values span all positive and negative values in the vicinity of the pole, the nonsingular part of the function yields a zero value in its vicinity. The poles can arise either from the first or from the third term of Eq. (46). When a negative energy changes in the vicinity of the bound state from the region below it to the region above the bound state, the corresponding wave function $\varphi_{ik}(r)$ changes its character in the vicinity of r_0 from exponentially increasing through exponentially decaying (at the exact energy of the bound state) to exponentially increasing with a node. For certain energy in this interval, $\varphi_{ik}(r_0)$ vanishes and the term $1/R$ possesses a pole. Therefore, the first term of Eq. (46) yields a pole of $f_l(\kappa)$ in the vicinity of the bound states and their associated virtual states (due to the even symmetry of the R matrix along the κ axis). Apart from these narrow regions of κ , the first term of Eq. (46) does not yield any poles along the imaginary momentum axis.

It is a well-known property of the reverse Bessel polynomials that there are no real roots z_{lp} for even values of l and there is only one unpaired real zero z_{lp} for every odd l [41]. For $l = 1$, $\theta_1(z) = z + 1$ and the only root is $z_{11} = -1$. This implies that $f_1(\kappa)$ has a pole at $\kappa_P = -1/r_0$. As the first two terms of Eq. (46) smoothly depend on κ in the vicinity of κ_P , the presence of the pole implies an existence of an associated node of $f_1(\kappa)$ in the vicinity of κ_P . While its existence does not depend on any particular character of $V(r)$, its position does via the first term of Eq. (46). Therefore, the virtual state near the pole κ_P is due to the p -wave boundary condition.

Function $f_1(\kappa)$ calculated for the model potential (40) is for the vicinity of κ_P plotted in Fig. 4. Note that the position of the pole κ_P is not physically significant, since it depends on r_0 . Since the boundary condition (6) holds for any $r \geq r_0$, so does its form expressed in terms of $f_l(\kappa)$. Therefore, the nodes of $f_l(\kappa)$ do not depend on r_0 . The radial dependence due to the third term in Eq. (46) is compensated by the radial dependence of the R matrix in the first term.

The imaginary momentum of the virtual state of the model potential (40) calculated using Eq. (46) coincides with the momentum of the RVS. The approach presented above shows

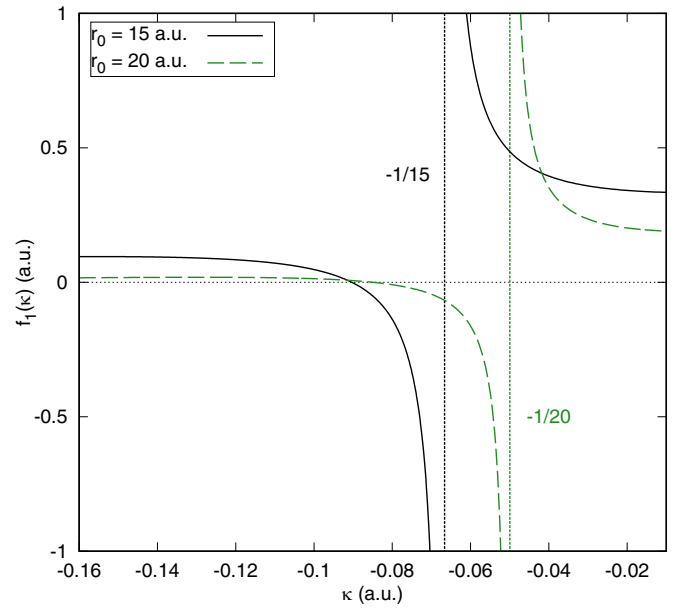


FIG. 4. Function $f_1(\kappa)$ calculated for the model potential (40) in the vicinity of the pole κ_P due to the third term of Eq. (46). The solid black line and dashed green (gray) line represent the results for $r_0 = 15$ a.u. and for $r_0 = 20$ a.u., respectively.

that a virtual state exists as a consequence of the properties of the spherical Hankel functions for a broad category of the short-range potentials. However, this discussion does not make its “resistance” against the scaling of the potential readily visible. Another example, discussed in Sec. V, shows that the RVSs also exist in a different category of interactions—separable potentials, along with the virtual states that are not associated with any bound states. However, in the case of the nonlocal separable potentials, these two types of states do not necessarily coincide.

E. Higher partial waves

The discussion of the pole of function $f_l(\kappa)$ [Eq. (46)] due to the outgoing-wave boundary condition presented in Sec. IV D for the p wave can be generalized in a straightforward way to every odd partial wave, since the reverse Bessel polynomials of the odd orders have a single unpaired real root.

As can be seen in Table I for the model potential (40), the virtual state that is not associated with the bound state exists in the partial waves p and f . The dependence of the f -wave RVS on the potential strength Λ is plotted in Fig. 5 along with the bound states and their associated virtual states. It shows that the virtual state that is not associated with the bound state is an RVS, similar to the one in the p wave (see Fig. 2).

On the other hand, the RVSs are not guaranteed to exist in the even partial waves as the reverse Bessel polynomials of the corresponding orders do not have any real roots. This corresponds to the absence of the additional virtual state in Table I for the d wave of the model potential (40). The RVS is also absent in the plot of the momenta of the d -wave virtual and bound states as a function of the potential strength Λ in Fig. 6.

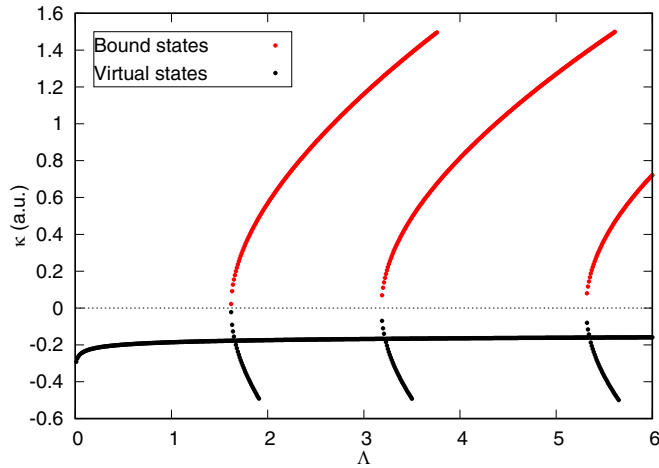


FIG. 5. The same quantities as in Fig. 2, here plotted for the partial wave f .

F. General perturbation

Previous sections have shown that energy of the RVS remains finite even when potential strength increases to infinity. It is important to mention that this property holds even for a perturbation that differs from the original interaction potential $V(r)$. We chose to demonstrate it on the potential (41),

$$V_l(r) = (ar^2 - b)e^{-cr^2} + \frac{l(l+1)}{2r^2} + \lambda U(r), \quad (47)$$

where $U(r)$ is a general perturbation. An example for

$$U(r) = -\frac{e^{-r}}{r} \quad (48)$$

and $l = 1$ is displayed in Fig. 7. Note that while Figs. 2 and 7 look similar they have different perturbation strengths as a variable on the x axis. Figure 2 refers to the global scaling parameter Λ in Eq. (42), whereas λ in Fig. 7 scales only the additional perturbation $U(r)$. Hence, the data in the figures coincide only for $\Lambda = 1$ and $\lambda = 0$.

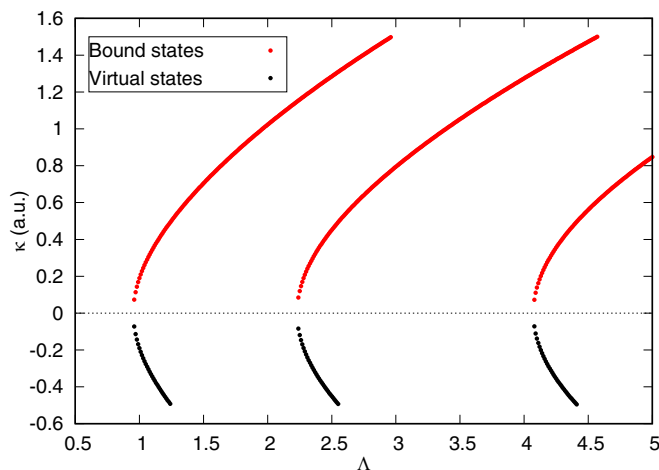


FIG. 6. The same quantities as in Fig. 2, here plotted for the partial wave d . The RVS is absent.

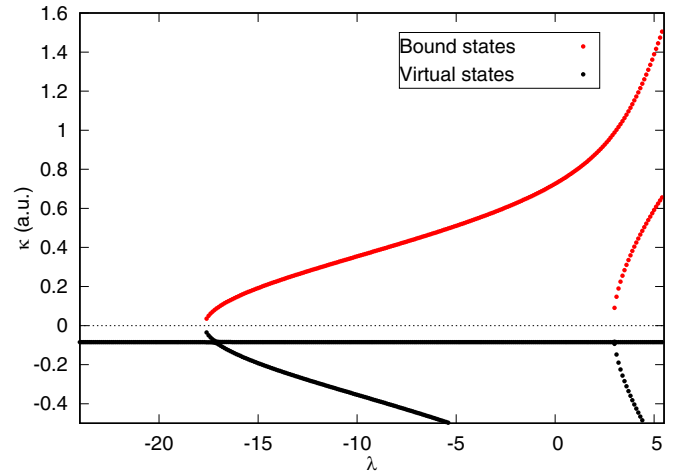


FIG. 7. Imaginary momentum $\kappa = -ik$ as a function of the dimensionless perturbation strength λ [see Eqs. (47) and (48)] and $l = 1$. The red dots $\kappa > 0$ represent the trajectories of the bound states; the black dots $\kappa < 0$ correspond to the trajectories of the virtual states.

V. RVS IN SEPARABLE POTENTIAL

While the potential (40) has a straightforward spatial character, advanced computational methods are necessary to accurately calculate the poles of its S matrix. A complementary set of potentials exist that can be constructed by fixing the complex momentum of a bound or a virtual state—separable potentials. Analysis of the near-threshold virtual states for a potential in this category provides a view on the RVSs that is complementary to the preceding sections.

An essential object in this analysis is the coupling function $\Lambda(\kappa)$ [42]. For an attractive potential V , it is defined as follows: A bound-state problem is solved for the scaled potential ΛV , where the value of Λ is sufficiently large to support a bound state. The pairs of varying values of Λ and corresponding eigenenergies E of the bound states define the real function $\Lambda(E)$. Using the relation $E = -\kappa^2/2$, this function can be written as $\Lambda(\kappa)$ for $\kappa > 0$.

To see the role of $\Lambda(\kappa)$ in the RVSs for $l > 0$, its analytical expression would be desirable. While it is not known for the local potentials discussed in the sections above, it is straightforward for the separable potentials. This problem has been studied, for example, by Kok and van Haeringen [43] as well as by Horáček and Pichl [44]. Consider a simple model Hamiltonian with a single separable interaction in a single partial wave l :

$$H_\Lambda = \frac{\mathbf{p}^2}{2} - |g\rangle \Lambda \langle g|, \quad (49)$$

where \mathbf{p} is a momentum operator and the form factor $|g\rangle$ satisfies the threshold law in the momentum representation [45]

$$g(p) \sim p^l, \quad (50)$$

where p is the eigenvalue of the operator \mathbf{p} . Solving the Schrödinger equation

$$H_\Lambda |\phi\rangle = -\frac{\kappa^2}{2} |\phi\rangle \quad (51)$$

TABLE II. Form factors $g_{ln}(p)$ from Eq. (53) for $l = 1, n = 0, 1, 2$ and corresponding coupling functions $\Lambda_{ln}(\kappa)$ obtained from Eq. (52) along with its asymptotic behavior for $\kappa \rightarrow \infty$.

n	$g_{ln}(p)$	$\Lambda_{ln}(\kappa)$	$\Lambda_{ln}(\kappa \rightarrow \infty)$
0	$\frac{p}{p^2 + a^2}$	$\frac{2(a + \kappa)^2}{(a + 2\kappa)}$	$\sim \kappa$
1	$\frac{p}{(p^2 + a^2)^{3/2}}$	$\frac{8a(a + \kappa)^3}{(a + 3\kappa)}$	$\sim \kappa^2$
2	$\frac{p}{(p^2 + a^2)^2}$	$\frac{16a^3(a + \kappa)^4}{(a^2 + 4a\kappa + \kappa^2)}$	$\sim \kappa^2$

for the bound states in the momentum representation with the normalization $\langle \phi | \phi \rangle = 1$ yields [43]

$$\frac{1}{\Lambda(\kappa)} = \frac{2}{\pi} \int_0^\infty \frac{p^2 g(p)^2}{p^2 + \kappa^2} dp. \quad (52)$$

This equation can be used in two ways: the energy of the bound state may be obtained for selected Λ or, vice versa, the potential strength can be calculated for given κ . Note that the separable interaction $\Lambda V = |g\rangle \Lambda \langle g|$ can provide at most one bound state. In the following the coupling function (52) is analytically continued to describe the virtual states ($\kappa < 0$) and resonances ($\kappa \in \mathbb{C}$).

A form factor, widely used in nuclear physics, is used here to demonstrate the RVSSs. It is of the form

$$g_{ln}(p) = \frac{p^l}{(p^2 + a^2)^{l+n/2}}, \quad (53)$$

where n is a nonnegative integer [45] and a is a real constant. Its explicit forms for $l = 1$ and three lowest values of n are listed in Table II along with corresponding coupling functions $\Lambda_n(\kappa)$ obtained from Eq. (52).

The functions $\Lambda_{ln}(\kappa)$ in Table II show different asymptotic behavior for $\kappa \rightarrow \infty$. The function $\Lambda_{10}(\kappa)$ increases linearly, whereas the functions $\Lambda_{ln}(\kappa) \sim \kappa^2$ asymptotically for $n > 0$ (even for higher n than considered here). The potentials (53) by Mongan [45] with the lowest values of n have been selected for this study due to the fact that the asymptotic character of their coupling functions $\Lambda_{ln}(\kappa)$ reflects the behavior of $\Lambda(\kappa)$ for the local potentials. It has been shown by Bárta and Horáček [46] that $\Lambda(\kappa) \sim \kappa^2$ for all finite local potentials, whereas for the local potentials with a singularity, $\Lambda(\kappa) \sim \kappa$, as in the case of potential with the $g_{10}(p)$ form factor introduced above.

It is clear that the coupling function $\Lambda(\kappa)$ here fits the same role as the interaction strength used for the local potential (42). Since the coupling function $\Lambda(\kappa)$ is known, inversion of the formulas listed in the third column of Table II reveals a dependence of the roots κ on the potential strength Λ . In the case of $\Lambda_{10}(\kappa)$, two roots exist that represent a pair of one bound and one virtual state, a pair of resonances or two virtual states. Similarly, the function $\Lambda_{11}(\kappa)$ yields three roots, $\Lambda_{12}(\kappa)$ yields four roots, etc.

Let us now discuss in detail the separable potential with the form factor $g_{11}(p)$. The corresponding coupling function $\Lambda_{11}(\kappa)$ is of the third order (see Table II), and the equation for

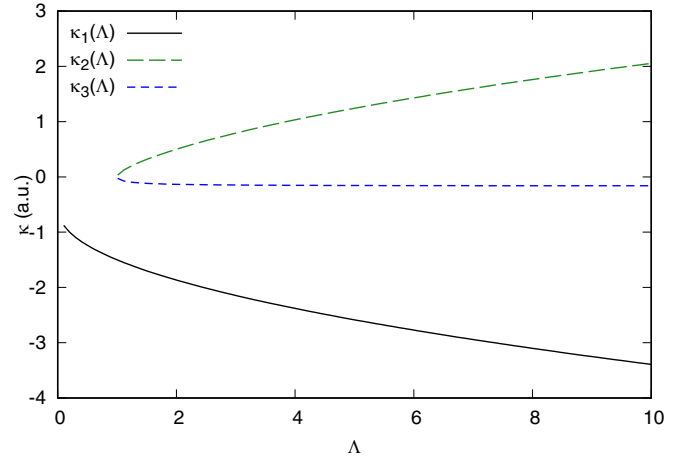


FIG. 8. Imaginary momentum κ_2 of the bound state and imaginary momenta κ_1, κ_3 of the virtual states for the separable potential with the form factor (53) as a function of the coupling constant Λ .

the eigenmomenta yields

$$\Lambda_{11}(\kappa) = \frac{8a(a + \kappa)^3}{(a + 3\kappa)} = \Lambda. \quad (54)$$

The solutions κ_1, κ_2 , and κ_3 can be explicitly written as

$$\kappa_1(\Lambda) = -\frac{1}{2} \left(\frac{q}{2^{2/3}a} + 2a + \frac{\Lambda}{\sqrt[3]{2}q} \right), \quad (55)$$

$$\kappa_2(\Lambda) = \frac{(1 - i\sqrt{3})q}{4 \cdot 2^{2/3}a} - a + \frac{(1 + i\sqrt{3})\Lambda}{4\sqrt[3]{2}q}, \quad (56)$$

and

$$\kappa_3(\Lambda) = \frac{(1 + i\sqrt{3})q}{4 \cdot 2^{2/3}a} - a + \frac{(1 - i\sqrt{3})\Lambda}{4\sqrt[3]{2}q}, \quad (57)$$

where

$$q(\Lambda) = \sqrt[3]{4a^3\Lambda + \sqrt{2}\sqrt{8a^6\Lambda^2 - a^3\Lambda^3}}. \quad (58)$$

These solution may represent (1) one bound state and a resonance pair, (2) one bound state and two virtual states, or (3) three virtual states. They show different behavior as $\Lambda \rightarrow \infty$. Specifically, κ_3 remains finite,

$$\lim_{\Lambda \rightarrow \infty} \kappa_3(\Lambda) = -\frac{a}{3}, \quad (59)$$

while the remaining roots increase to infinity as $\kappa_{1,2}(\Lambda) \sim \sqrt{\Lambda}$. The finite limit of κ_3 corresponds to the pole of the coupling function $\Lambda_{11}(\kappa)$ in Eq. (54). All three roots $\kappa_1(\Lambda), \kappa_2(\Lambda), \kappa_3(\Lambda)$ are shown in Fig. 8 for $a = 0.5$. The figure reveals, that the separable potential with the form factor g_{11} provides one VS for $0 < \Lambda < 1$ before the resonant pair is transformed into the bound and virtual pair. However, in contrast to the case of the local potential Eq. (41) discussed in the previous section, this single low- Λ pole is not the RVS. The resistant VS in this case is the virtual state that appears in pair with the bound state once the interaction becomes strong enough to support the bound state, i.e., for $\Lambda > 1$.

VI. CONCLUSIONS

The first conclusion of this article is Eq. (39). It is an expression of the scattering length—an essential parameter of the low-energy short-range scattering—only in terms of the poles of the S matrix for an arbitrary angular momentum $l > 0$. This formula confirms that the low-lying resonances and weakly bound states greatly affect the scattering cross section in the limit of low collision energy. Furthermore, it quantifies the contribution of the near-threshold virtual states. In the absence of the low-lying resonances and weakly bound states, these can have a dominant and essential effect on the scattering length.

This was demonstrated on the short-range potential (40) introduced by Davis and Sommerfeld [36] in the p wave. The near-threshold poles of its S matrix were calculated, and it was shown that the scattering length is dominated by a low-lying virtual state. However, this virtual state was not associated with any bound state, as is usual in the case of the short-range local potentials with $l > 0$. Its position in the complex momentum plane as a function of the potential strength was analyzed to assess whether it turns into a bound state or a resonance as the potential becomes increasingly more and less attractive, respectively. This S -matrix pole not only does not move away from the negative imaginary momentum semiaxis, it shows only very weak dependence on the potential strength. To the best of our knowledge, virtual states with this behavior (referred to as resistant virtual states) have not been previously reported.

Further analysis presented in this article revealed that the appearance of the RVS is a rather general phenomenon. A single RVS is present in every odd partial wave for every local short-range potential. It is a consequence of the outgoing-wave boundary condition and analytical properties of the spherical Hankel functions' linear combination, which forms the solution of the Schrödinger equation in the asymptotic region. The position of its momentum on the negative imaginary axis is affected by the details of the interaction potential.

While all the analysis of the RVSs in this article was presented for the case of a local short-range potential in the X representation, the example in Sec. V shows that they can also be supported by separable potentials. In this example, however, a virtual state supported even in the absence of any bound state is different from the RVS that appears only at such strength of the interaction that allows one state to be bound. While this structure of the virtual states is different from the local interaction, it suggests that the phenomenon of the RVSs is more general than the scope of the discussion presented here.

ACKNOWLEDGMENT

This work was supported by the Czech Science Foundation (Grant No. GACR 21-12598S).

APPENDIX: METHOD OF CALCULATION OF BOUND AND VIRTUAL STATES

The energies of the bound and virtual states can be easily found using a simple integral equation. The Lippmann-Schwinger equation can be written in the coordinate representation as follows [37]:

$$\psi_l(r) = \hat{j}_l(kr) - \frac{i}{k} \hat{j}_l(kr) \int_r^\infty \hat{h}_l^{(1)}(kr') 2V(r') \psi_l(r') dr' - \frac{i}{k} \hat{h}_l^{(1)}(kr) \int_0^r \hat{j}_l(kr') 2V(r') \psi_l(r') dr', \quad (\text{A1})$$

where $\hat{j}_l(kr)$ and $\hat{h}_l^{(1)}(kr)$ are the spherical Riccati-Bessel and Riccati-Hankel functions, respectively. Note that Taylor [37] employs Hankel functions $\hat{h}_l^{(+)} = i\hat{h}_l^{(1)}$, where the definition of $\hat{h}_l^{(1)}$ can be found in Ref. [47]. At large values of r , where the interaction $V(r)$ is negligible, this equation yields

$$\psi_l(r) = \hat{j}_l(kr) - i\hat{h}_l^{(1)}(kr)T_l(k), \quad (\text{A2})$$

where

$$T_l(k) = \frac{1}{k} \int_0^\infty \hat{j}_l(kr) 2V(r) \psi_l(r) dr. \quad (\text{A3})$$

Equation (A1) can be transformed into the Volterra-type integral equation [37]

$$\phi_l(r) = \hat{j}_l(kr) + \frac{i}{k} \int_0^r [\hat{j}_l(kr)\hat{h}_l^{(1)}(kr') - \hat{j}_l(kr')\hat{h}_l^{(1)}(kr)] \times 2V(r')\phi_l(r') dr' \quad (\text{A4})$$

that can be very accurately solved using the Romberg extrapolation technique as described in Refs. [38,48]. Different boundary conditions of the solution $\phi_l(r)$ lead to a different expression for the T matrix:

$$T_l(k) = \frac{\frac{1}{k} \int_0^\infty \hat{j}_l(kr) 2V(r) \phi_l(r) dr}{1 + \frac{i}{k} \int_0^\infty \hat{h}_l^{(1)}(kr) 2V(r) \phi_l(r) dr}. \quad (\text{A5})$$

The poles of the T matrix are determined by the equation

$$1 + \frac{i}{k} \int_0^\infty \hat{h}_l^{(1)}(kr) 2V(r) \phi_l(r) dr = 0. \quad (\text{A6})$$

Equation (A4) is, in general, complex. However, for calculations of the bound and virtual states (for pure imaginary momentum) it can be trivially transformed into a real equation and the solution $\phi_l(r)$ then becomes a real function.

- [1] H.-W. Hammer, S. König, and U. van Kolck, *Rev. Mod. Phys.* **92**, 025004 (2020).
 [2] C. Bertulani, H.-W. Hammer, and U. van Kolck, *Nucl. Phys. A* **712**, 37 (2002).
 [3] J. Braun, H.-W. Hammer, and L. Platter, *Eur. Phys. J. A* **54**, 196 (2018).

- [4] C. Chin, R. Grimm, P. Julienne, and E. Tiesinga, *Rev. Mod. Phys.* **82**, 1225 (2010).
 [5] L. P. Benofy, E. Buendía, R. Guardiola, and M. de Llano, *Phys. Rev. A* **33**, 3749 (1986).
 [6] D. Field, N. C. Jones, S. L. Lunt, and J.-P. Ziesel, *Phys. Rev. A* **64**, 022708 (2001).

- [7] D. Field, N. C. Jones, and J.-P. Ziesel, *Phys. Rev. A* **69**, 052716 (2004).
- [8] M. A. Morrison, *Phys. Rev. A* **25**, 1445 (1982).
- [9] L. A. Morgan, *Phys. Rev. Lett.* **80**, 1873 (1998).
- [10] C.-H. Lee, C. Winstead, and V. McKoy, *J. Chem. Phys.* **111**, 5056 (1999).
- [11] T. N. Rescigno, D. A. Byrum, W. A. Isaacs, and C. W. McCurdy, *Phys. Rev. A* **60**, 2186 (1999).
- [12] S. Mazevet, M. A. Morrison, L. A. Morgan, and R. K. Nesbet, *Phys. Rev. A* **64**, 040701(R) (2001).
- [13] I. I. Fabrikant, *J. Phys. B: At. Mol. Phys.* **17**, 4223 (1984).
- [14] A. K. Kazansky, *J. Phys. B: At. Mol. Phys.* **16**, 2427 (1983).
- [15] A. Herzenberg, in *Electron-Molecule Collisions*, edited by I. Shimamura and K. Takayanagi (Plenum Press, New York, 1984), pp. 191–274.
- [16] H. Estrada and W. Domcke, *J. Phys. B: At. Mol. Phys.* **18**, 4469 (1985).
- [17] W. Vanroose, Z. Zhang, C. W. McCurdy, and T. N. Rescigno, *Phys. Rev. Lett.* **92**, 053201 (2004).
- [18] J. Dvořák, M. Ranković, K. Houfek, P. Nag, R. Čurík, J. Fedor, and M. Čížek, *Phys. Rev. Lett.* **129**, 013401 (2022).
- [19] J. Dvořák, M. Ranković, K. Houfek, P. Nag, R. Čurík, J. Fedor, and M. Čížek, *Phys. Rev. A* **106**, 062807 (2022).
- [20] Y. N. Demkov and G. F. Drukarev, *Sov. Phys. JETP* **22**, 479 (1966).
- [21] O. I. Tolstikhin, V. N. Ostrovsky, and H. Nakamura, *Phys. Rev. A* **58**, 2077 (1998).
- [22] P. A. Batishchev and O. I. Tolstikhin, *Phys. Rev. A* **75**, 062704 (2007).
- [23] A. J. F. Siegert, *Phys. Rev.* **56**, 750 (1939).
- [24] A. Sitenko, *Lectures in Scattering Theory* (Pergamon Press, Oxford, 1971).
- [25] F. W. J. Olver, D. W. Lozier, R. F. Boisvert, and C. W. Clark, *The NIST Handbook of Mathematical Functions* (Cambridge University Press, New York, 2010).
- [26] E. Grosswald, *Bessel Polynomials* (Springer, Berlin, 1978).
- [27] R. Newton, *Scattering Theory of Waves and Particles* (McGraw-Hill, New York, 1966).
- [28] H. Edwards, *Galois Theory* (Springer, New York, 1997).
- [29] V. Prasolov and D. Leites, *Polynomials* (Springer, Berlin, Heidelberg, 2004).
- [30] S. Winder, *Analog and Digital Filter Design* (Newnes, 2002).
- [31] M. E. H. Ismail and D. H. Kelker, *SIAM J. Math. Anal.* **7**, 82 (1976).
- [32] Ş. Yüzbaşı and M. Sezer, *Appl. Math. Comput.* **219**, 10610 (2013).
- [33] H. Krall and O. Frink, *Trans. Amer. Math. Soc.* **65**, 100 (1949).
- [34] S. Ahmed, *J. Approx. Theory* **45**, 288 (1985).
- [35] A. Amaya-Tapia, S. Y. Larsen, J. Baxter, M. Lassaut, and M. Berrondo, *Mol. Phys.* **100**, 2605 (2002).
- [36] J. U. Davis and T. Sommerfeld, *Eur. Phys. J. D* **75**, 316 (2021).
- [37] J. Taylor, *Scattering Theory: The Quantum Theory of Nonrelativistic Collisions* (Dover Publications, New York, 2006).
- [38] M. Čížek and J. Horáček, *J. Phys. A: Math. Gen.* **29**, 6325 (1996).
- [39] M. Aymar, C. H. Greene, and E. Luc-Koenig, *Rev. Mod. Phys.* **68**, 1015 (1996).
- [40] P. Burke, *R-Matrix Theory of Atomic Collisions: Application to Atomic, Molecular and Optical Processes* (Springer, Heidelberg, 2011).
- [41] M. de Bruin, E. Saff, and R. Varga, *Indagationes Math.* **84**, 1 (1981).
- [42] V. I. Kukulin, V. M. Krasnopolsky, and J. Horáček, *Theory of Resonances* (Kluwer Academic, Dordrecht, 1989).
- [43] L. Kok and H. van Haeringen, *Ann. Phys.* **131**, 426 (1981).
- [44] J. Horáček and L. Pichl, *Commun. Comput. Phys.* **21**, 1154 (2018).
- [45] T. R. Mongan, *Phys. Rev.* **175**, 1260 (1968).
- [46] T. Bárta and J. Horáček, *Phys. Scr.* **95**, 065401 (2020).
- [47] S. Flügge, *Practical Quantum Mechanics* (Springer-Verlag, New York, 2012).
- [48] J. Horáček and J. Bok, *Comput. Phys. Commun.* **59**, 319 (1990).